

various mediums $x = \Gamma^{n,n+1}$. The indexes n, s, ℓ, ν stand for the n -th material and the solid, liquid phases and the evaporated phases.

The combined variant of Stefan problem is used for the mathematical description of thermal processes and phase transitions in multilayered materials. The heating and melting-solidification are characterized by the classical Stefan problem for each layer based on a nonlinear heat conduction equation and surface evaporation is described by a single-phase variant of Stefan problem:

$$\left[\frac{\partial(\rho H)}{\partial t} = \frac{\partial}{\partial x} \lambda(T) \frac{\partial T}{\partial x} \right]_k, \quad H = C_p(T) \cdot T \quad k = s, \ell \quad n = 1, 2, 3 \quad x_0 < x < \Gamma_{kv}(t), \quad t > 0. \quad (1)$$

The following initial and boundary conditions were used:

$$t = t_0 : T(t_0, x) = T_0, \quad x = x_0 : \left[-\lambda(T) \frac{\partial T}{\partial x} = 0 \right] \quad (2)$$

The differential Stefan condition and continuity of temperatures are used at the solid-liquid interphase boundaries $x = I_{st}^n(t)$:

$$x = I_{st}^n(t) : \left[\lambda_s(T) \frac{\partial T_s}{\partial x} - \lambda_l(T) \frac{\partial T_l}{\partial x} = \rho_s L_m \nu_{st} \right]_k, \quad [T_{st} - T_s = T_l = T_m]^n, \quad n = 1, 2, 3 \quad (3)$$

The conditions of ideal contact are used at the contact boundaries at $x = \Gamma^{n,n+1}$:

$$x = \Gamma^{n,n+1} : \left[\lambda(T) \frac{\partial T}{\partial x} \right]^- - \left[\lambda(T) \frac{\partial T}{\partial x} \right]^{n+1}, \quad n = 1, 2, 3 \quad T^n = T^{n+1} \quad (4)$$

The surface evaporation was described using an approach of the Knudsen layer at the right irradiated boundary $x = \Gamma_{kv}^n(t)$, ($k = s, \ell$):

$$x = I_{kv}^n(t) : \left[\lambda_k(T) \frac{\partial T_k}{\partial x} \cdot A(T_k) \cdot G + \rho_k L_\nu \nu_{kv} \right]_k, \quad [\rho_k \nu_{kv} = \rho_\nu (\nu_{kv} - u)]^n, \quad [P_k + \rho_k \nu_{kv}^2 = P_\nu + \rho_\nu (\nu_{kv} - u)^2]^n, \quad (5)$$

$$[T_\nu = \alpha_T(M) T_k]^n, \quad [\rho_\nu = \alpha_\rho(M) \cdot \rho_H]^n, \quad \left[\rho_H = \frac{P_H(T_k)}{RT_k} \right]^n, \quad \left[P_H(T_k) = P_b \exp \left[\left(\frac{1}{T_b} - \frac{1}{T_k} \right) \frac{L_v}{R} \right] \right]^n, \quad (6)$$

where at $M = 1 : \alpha_T(M) = 0.633, \alpha_\rho(M) = 0.326$, at $M = 0 : \alpha_T(M) = \alpha_\rho(M)$,

T_k is the condensed matter temperature, $\alpha_T(M), \alpha_\rho(M)$ are the Crout coefficients, M is Mach number, R is gas constant, ρ_H, P_H are the density and pressure of saturated vapor, $\lambda(T)$ is heat conductivity, $C_p(T)$ is heat capacity, H is enthalpy, L_m, L_ν is transition heat for melting and evaporation accordingly, ν_{st}, ν_{kv} are the velocity of melting-solidification and evaporation fronts, $A(T)$ is absorption coefficient, $\rho(T), P(T), u$ are density, pressure and velocity of sound accordingly, T_b, T_m are the temperatures of boiling and melting.

3 ALGORITHM OF THE SOLUTION

The numerical solution of mathematical model (1) - (6) was performed using the dynamic adaptation method which is based on the transition to an arbitrary non-stationary coordinate system with variables (q, τ) . The unknown variables in such transition include not only the grid

functions T_i^j , but also coordinates of the grid nodes x_i^j . The backward transformation equation representing partial differential equation is used for their definition. The equation is constructed in such a manner that the nodes movement velocity depends on the dynamics of the solution of the equations describing the physical processes. The transition from the physical $\Omega_{x,t}$ into computational $\Omega_{q,\tau}$ space is carried out by means of change of variables $x = \xi(q, \tau), t = \tau$ with

backward non-degenerate transformation $q = \varphi(x, t)$, $\tau = t$. The mathematical statement of the initial problem (1-6) in new variables (q, τ) takes the form:

$$\left[\frac{\partial(\psi H)}{\partial \tau} = -\frac{\partial(HQ)}{\partial q} - \frac{\partial W}{\partial q} \right]_k, \quad H = C_p T, \quad \left[W = -\frac{\lambda(T)\rho}{\psi} \frac{\partial T}{\partial q} \right]_k, \quad (7)$$

$$\left[\frac{\partial \psi}{\partial \tau} = \frac{\partial Q}{\partial q} \right]_k, \quad \left[\frac{\partial x}{\partial q} = \frac{\psi}{\rho} \right]_k, \quad q_0 < q < \Gamma_{kv}, \quad \tau \geq 0, \quad (8)$$

The equation (8) is used to construct the adaptive grid after the definition of the specific form of the function Q . The differential analogue of this equation describes the dynamics of the grid nodes, and the function Q carries out controllable movement of the grid nodes coordinated with dynamics of the sought solution.

Additional equation (8) requires additional initial and boundary conditions:

$$\tau = \tau_0: \quad \psi(\tau_0, q) = 1, \quad (9)$$

$$q = q_0: \quad Q(\tau, q_0) = 0 \quad (10)$$

$$q = I_{si}^n: \quad [T_{si} - T_s = T_l - T_m]^n, \quad Q_{si}^n = -\rho_s v_{si}^n = \left\{ \left[\lambda(T) \frac{\rho}{\psi} \frac{\partial T}{\partial q} \right]_i \left[\lambda(T) \frac{\rho}{\psi} \frac{\partial T}{\partial q} \right]_s \right\} \cdot (I_m^n)' \quad (11)$$

$$q = I^{n+1}: \quad \left[\lambda(T) \frac{\rho}{\psi} \frac{\partial T}{\partial q} \right] = \left[\lambda(T) \frac{\rho}{\psi} \frac{\partial T}{\partial q} \right]^{n+1}, \quad T^n - T^{n+1}, \quad Q^{n+1}(\tau, I^{n+1}): 0 \quad (12)$$

Three conservation laws were used on the right evaporation boundary $q = I_{kv}^n$ ($k = s, l$)

$$q = I_{kv}^n: \quad \left[\lambda_k(T) \frac{\rho}{\psi} \frac{\partial T_k}{\partial q} = A(T_k) G - L_v Q_{kv} \right]^n, \quad \left[Q_{kv} = \rho_v \left(\frac{Q_{kv}}{\rho_k} + u \right) \right]^n, \quad \left[P_k + \frac{Q_{kv}}{\rho_k} = P_v + \rho_v \left(-\frac{Q_{kv}}{\rho_k} + u \right) \right]^n \quad (13)$$

where Q_{si} , Q_{kv} are the material flow over the solid-liquid and liquid-vapor boundaries. Three additional conditions (6) were used on the external boundary of Knudsen layer.

Semi-uniform distribution of the grid nodes in the method of dynamic adaptation is achieved from semi-uniform distribution of the function ψ which, in turn is achieved by proper selection of the transformation function Q from the diffusive approximation: $Q = -D \frac{\partial \psi}{\partial q}$, where D has the

meaning of diffusion coefficient and is determined by the parameters of the problem: the domain size $L(t)$ and boundary velocities v_0, v_r [2]:

$$D = \frac{L^2(t)}{\Delta L(t)} (v_r - v_0) = \frac{\psi L_0^2}{\Delta q \rho} (v_r - v_0) \quad (14)$$

Thus, the statement of the problem (7) – (14) does not include any fitting coefficients. This allows fully automated generation of semi-uniform grids with no regard to the linear size of the domain and boundary velocities.

4 MODELING RESULTS

The stated above method was used for numerical solution of the pulsed laser doping ($G = 3 \cdot 10^5 \dots 3 \cdot 10^4$ W/cm², $\tau_L = 1.5$ s) of Aluminum target ($\ell_{Al} = 0.5 \pm 1$ cm) with different sequences of thin layers of Cr and Ni ($\ell_{Ni} = \ell_{Cr} = 10-50$ mkm) ($\ell_{Al} = 0.5 \pm 1$ cm), according to the scheme at Fig. 1a,b. Computational grids with 30-40 nodes for solid and 20-30 for liquid phases were constructed in each sub-domain of the three-layer domain. The grid nodes within each layer were concentrated near the contact boundary. The dynamics of the melting and evaporation process of each layer is characterized by time distribution of velocity V_{sl} и V_{lv} and space distribution of ψ_s, ψ_l . The latter shows the change of the spatial size of solid and liquid phases under the influence of the moving melting fronts (Fig.2 a, b). The spatial size of the physical and computational space are equal at the

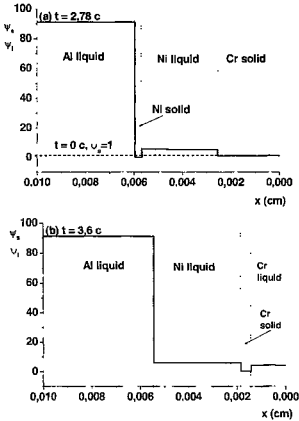


Fig. 2.

initial point $t=0$ so that the function $\psi_s(0,x)=1$, Fig. 2a (dotted line). Solid phase vanishes during melting of Aluminum (Fig 2 a, solid line), while $\psi_s(t,x)$ changes from 1 to 0. The liquid region reaches its maximum size $\psi_{\ell,Al}(t,x) \approx 92$. The moment $t = 2.78s$, Fig. 2 a, (solid line) corresponds to complete melting of the bottom layer of Al, melting over the middle layer of Ni and solid Cr. Fig. 2b shows spatial distribution of $\psi_s(t,x)$, $\psi_\ell(t,x)$ at $t = 3.6s$ that correspond to complete melting of Al and Ni and to the process of melting of Cr and is characterized by the relations $\psi_{s,Cr}(t,x) \ll 1$, $\psi_{\ell,Cr}(t,x) \gg 1$.

Fig. 3a, b show time profiles of melting and evaporation velocity for all materials. The situations at Fig. 3a и 3b correspond to the scheme of the processes at Fig. 1a и 1b.

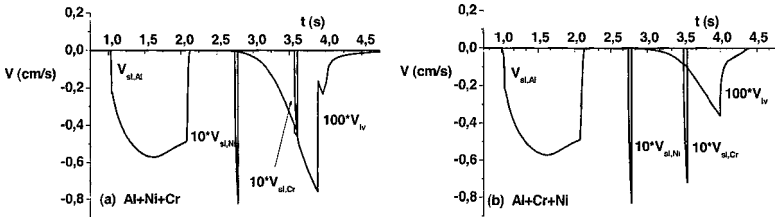


Fig. 3.

5 CONCLUSIONS

1. The suggested method of dynamic adaptation allows performing mathematical modeling of phase transitions dynamics in multilayer systems using low number of grid nodes.
2. The suggested method of determination of the diffusion coefficient allows computation of multi-front Stefan problems without fitting parameters.
3. Three-layer system never reaches stationary state regardless of the time profile and duration of the laser radiation.

REFERENCES

- [1] V.I. Mazhukin, A.A. Samarskii, M.M. Chuiko. Method of dynamic adaptation for the numerical solution of non-stationary multidimensional Stefan problem. Dokl. RAS, 1999, v.368, No 3, pp. 307-310.
- [2] O.N. Koroleva, V.I. Mazhukin. Mathematical simulation of laser induced melting and evaporation of multilayer materials/ Comp. Math. and Math. Phys, 2006, v. 46 No 5, pp. 848-862.